Hindawi
Journal of Chemistry
Volume 2019, Article ID 1805280, 6 pages
https://doi.org/10.1155/2019/1805280

Research Article

Synthesis, Characterization, and Thermal Behavior of Nanoparticles of $Mg(OH)_2$ to Be Used as Flame Retardants

A. A. Hanna, A. S. Abdelmoaty, and M. A. Sherief

Inorganic Chemistry Department, National Research Centre, P.O. Box: 12622, Dokki 11787, Egypt

Correspondence should be addressed to M. A. Sherief; gohamora@yahoo.com

Received 14 November 2018; Revised 21 January 2019; Accepted 3 June 2019; Published 17 June 2019

Academic Editor: Darren Sun

To study the effects of the precursor materials on the structure, the morphology, and the thermal stability of $Mg(OH)_2$ particles, five samples were prepared by using the same method. The produced powder was characterized by using FTIR, XRD, SEM, and TEM, and the thermal stability was studied by using the thermogravimetric analysis. This study aims to use the advantage prepared material as a flame-retardant for the polymeric materials. The characterization of the obtained samples shows that $Mg(OH)_2$ is formed in hexagonal phase and arranged in different shapes. The analysis of the data obtained from the TGA shows that $Mg(OH)_2$ in general decomposed in three steps, the first one due to the water content and the other volatile materials, the second step represents the decomposition of $Mg(OH)_2$ to produce MgO, and the third step represents the conversion of MgO to glassy layer. The samples prepared in presence of the surfactants gave a higher value for the formation of the glassy layer so that it is recommended to use this sample as flame retardant for the polymeric materials.

1. Introduction

The polymer materials were used successfully in different applications because they have excellent chemical, mechanical, and electrical properties [1–8]. The polymer materials have two main drawbacks: the first one is their flammability and the thermal degradation which represent environmental pollution and the second one is smoke that consists of many toxic gases such as nitrogen oxides from polyamides and CO_2, CO due to firing the organic materials, and the others due to their low melting point [9]. These gases resist the work of the firemen because of the creation of an atmosphere loaded with smoke. For these reasons, the polymer materials must be modified to overcome these defects. This modification goes in two directions, improving the properties of the polymer materials and adding some flame-retardant materials.

The most common flame-retardant materials are the halogenated or phosphorus compounds. These compounds commonly produce some toxic gases. On the other hand, the inorganic flame-retardant materials are the more acceptable compounds because they are hydrated materials which produce water vapour at low temperature and produce some oxides such as MgO, SiO_2, and Al_2O_3 which work as flame-retardant materials and work as smoke suppressants [10] at high firing temperature. Furthermore, their properties could absorb the evolved toxic gases such as CO, CO_2, SO_2, and nitrogen gases [5]. Among the inorganic flame-retardant materials, $Mg(OH)_2$ draws special attention of different authors [11–15] because it contains hydrated molecules when decomposed thermally at low temperature and its addition improves the mechanical properties of the polymers [16]. The effect of adding $Mg(OH)_2$ on the flammability of polymers focused on the structure and the shape of the produced $Mg(OH)_2$ powder. Henrist et al. and other works [17] found that the structure, the morphology, the size and agglomerations, and the thermal behavior of $Mg(OH)_2$ were influenced greatly by the method of preparation and their conditions as well as the precursor materials.

The aim of this work is concerned with the preparation of the nanoparticles of $Mg(OH)_2$ by using different precursor materials under different conditions and study of the thermal behaviors of the produced samples to be used as

flame-retardant materials. Also, the work discussed the growth and the nucleation of the produced phases.

2. Experimental

2.1. Preparation of $Mg(OH)_2$ Samples. Sixteen grams of NaOH, 1 g urea, and 8 ml ethanol are dissolved in a flask containing 50 ml deionized water; then, 50 ml $MgCl_2$ solution was added dropwise with stirring for 10 min at 60°C for 1 h and then kept for 10 h. The precipitate was washed and dried at 60°C. Five samples were prepared as shown in Table 1[18].

2.2. Characterization of the Produced Samples. The five prepared samples were characterized by using different techniques as follows.

2.2.1. X-Ray Diffraction (XRD) Analysis. X-ray diffraction (XRD) patterns were obtained with a power D8 ADVANCE diffractometer (Germany) using CuKa radiation (1.542°A, 40 KV, 40 mA) in the 2Θ range of 4–80. The acquisition parameters were a step size of 0.02 and a step time of 0.4 s.

2.2.2. Fourier Transform Infrared (FTIR) Spectroscopy. FTIR spectra of the samples were obtained using a KBr disk technique and FTIR 6500 spectrometer (JASCO, Japan) in the range of 400–4000 cm^{-1}.

2.2.3. Scanning Electron Microscope (SEM). The surface morphologies of the samples were carried out using a JEOL JSM t20 scanning electron microscope (SEM) (JEOL, Japan) at an accelerating voltage of 5 kV.

2.2.4. Transmission Electron Microscope (TEM). The morphology and the particle size of the prepared samples were examined by using a transmission electron microscope (TEM) Joel JEM 1230 working at 100 keV.

2.2.5. Thermal Analysis. The thermal analysis (TGA) was performed by using a USA Perkin–Elmer thermogravimeter. Samples of approximately 10 mg were heated from 50°C to 1000°C with heating rate 10/m under a nitrogen atmosphere, and the flow of nitrogen was 50 ml/min.

3. Results and Discussion

3.1. Fourier Transform Infrared (FTIR) Spectroscopy. Figure 1 (A, B, C, D, and E) illustrates the IR spectrum of the five prepared samples. The IR profiles of these samples behave the same trends and are similar to those reported in the literature [19]. The IR curves indicate that there are some changes in the intensity and the sharpness of the peaks while slight change in their position according to the start materials. For sample A, it is observed that the intensity of the peaks is smaller than that of other samples. These findings are in agreement with the literature [18, 20]. This means that the

Table 1: Start materials for preparation of the samples.

Samples	NaOH (g)	$MgCl_2$ (ml)	Urea (g)	Ethanol (ml)	Ethylene glycol (ml)	CTAB (g)
A	16	50	1	8	—	—
B	16	50	1	—	—	—
C	16	50	—	8	—	—
D	16	50	1	8	8	—
E	16	50	1	8	—	2

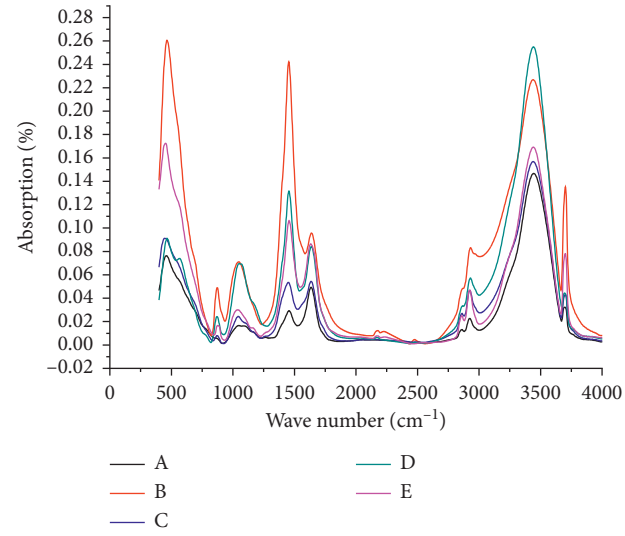

Figure 1: FTIR of prepared samples.

presence of the urea and the solvent can prevent the growth of the $Mg(OH)_2$ crystals while they help in the formation of the crystals. So, the structure and the morphology of the prepared $Mg(OH)_2$ are controlled by the precursor material, the method of preparation, and its conditions as suggested by Henrist and Yang [17, 21]. The IR spectra of the samples E and B show that the intensity and sharpness of the peaks were increased; the presence of the surfactants improves the growth of the crystals of the $Mg(OH)_2$ as reported previously [18]. On the other hand, the absence of the solvent restricted the nucleation and improves the growth of the crystals. For samples C and D, there are no effects observed. This means that the absence of urea and the presence of the gelating agent help in the formation and nucleation of the crystals. In general, for all samples, the IR charts indicate the formation of $Mg(OH)_2$ as follows:

(i) The appearance of the remarkable sharp and intense peak at 3600 cm^{-1} is assigned to the OH antisymmetric stretching vibration in the $Mg(OH)_2$ [22]

(ii) The appearance of the two peaks at 3450 cm^{-1} and 1635 cm^{-1} could be due to the stretching vibration and the bending vibration of the water molecules, respectively

(iii) The appearance of the absorption peak at 500 cm^{-1} may due to the stretching vibration of Mg-O

(iv) The appearance of previous peaks indicates that $Mg(OH)_2$ crystals were formed in all the cases [23]

3.2. X-Ray Diffraction (XRD). The XRD patterns of the prepared samples are illustrated in Figure 2 (A, B, C, D, and E); the main diffraction peaks corresponding to the hexagonal phase of $Mg(OH)_2$ according to JCPDS card no. 7-239 appeared. The XRD patterns show some changes in the intensity of peaks depending on the precursor materials.

For sample A, small peaks appeared at 2 theta 17 cm^{-1}, 28 cm^{-1}, 33 cm^{-1}, 37 cm^{-1}, 47 cm^{-1}, 57 cm^{-1}, and 67 cm^{-1}. For sample B, the sharpness of the special peaks increases; this means that the growth of the formed crystals increases. For samples C and D, the sharpness of the specified peaks increased but was less than that of sample B. For sample E, which contains the surfactants (CTAB), the sharpness of the specified peaks increased greatly. From this result, it may be concluded that the growth and the nucleation of the crystals of $Mg(OH)_2$ depend on the precursor materials.

3.3. Scanning Electron Microscope (SEM) and Transmission Electron Microscope (TEM). To study the effects of the precursor materials on the morphology of the produced $Mg(OH)_2$, the scanning electron microscopy and the transmission electron microscopy were performed as shown in Figures 3 and 4 from A to E. For sample A (Figure 3(a)), the formed particles are hexagonal crystals with definite boundary where the presence of the solvent prevents the agglomeration for the particles. It is also observed that the formed particles were arranged randomly with different sizes. For sample B, the formed particles also have a hexagonal crystal and are arranged in layered structure (Figure 3(b)). For sample C which represents the reaction between the reactant materials without urea, the formed particles tend to form rod-like structures while the photo exhibits some agglomeration. For sample D, the SEM photo exhibits a well rod structure; this may be due to the ethylene glycol being used as a gelating agent. For sample E, which contains the surfactants, the SEM photo exhibits a regular structure with clear boundary. The TEM measurements are in agreement with the SEM photos as shown in Figures 4(a)–4(e). The TEM photos for all prepared samples indicate that the particle size are in the range of nanoparticles of about 5–10 nm.

3.3.1. Thermogravimetric Analysis (TGA). Thermogravimetric analysis (TGA) for the five prepared samples was used to evaluate the thermal behavior over the heat range between the room temperature and 1000°C. The thermal gravimetric profiles show that the samples C and E behave in the same trends as shown in Figure 5 (C and E) where the weight loss at the temperature below 500°C is about 2% and 5% for the sample C and sample E, respectively. As this stage represents the liberation of the water content, this means that the two samples contain some absorbed surface water. Also, the TG curves indicate that the residual content which represents the formation of the glassy layer from MgO is higher than in the other samples. Generally, it may characterize three stages of the thermal decomposition. The first one starts at the room temperature ending at 200°C; this stage may be attributed to the surface and the hydrated water. The second step starts at 200°C and ends at 480°C corresponding to the decomposition of $Mg(OH)_2$ to form MgO [24, 25]. The third step represents the firing of MgO, converting it to a glassy state and continuing till 1000°C with negligible weight loss. The appearance of the three stages was observed for all the samples with negligible weight loss at the starting and the ending temperature. The difference between the starting and ending temperatures may be due to the amount of the adsorbent water on the surface of the prepared particles and the structure and the shape of the prepared particles. This is confirmed from the percentage of weight loss of the residue amount at the temperature above 500°C. The difference between the residual percentages may be due to the adsorbed and the hydrated water and the other organic solvents which are used in the preparation as well as the shape of the crystals. The TG curves exhibit the formation of the MgO glassy phase which prevents the spread of the flame through the burning materials [25]. The residual for samples C and E is greater than for the other samples, and the residual contents follow the following arrangement E > C > A > B > D. This means that the samples C and E prepared by this method are more preferable for use as flame retardant for the polymeric materials. Also, the thermogravimetric curves indicate that $Mg(OH)_2$ is thermally stable in spite of the presence of the water and the method of preparation.

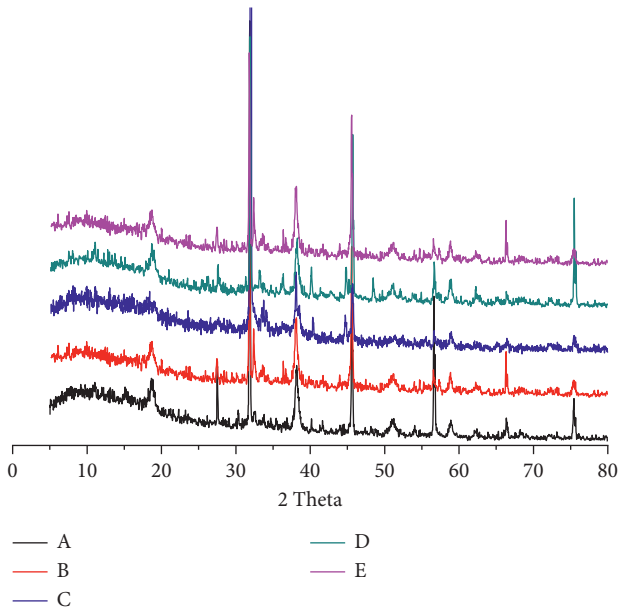

Figure 2: XRD of prepared samples.

4. Conclusion

From the analysis of the obtained results, it may be concluded that the formed nanoparticles of $Mg(OH)_2$ have a hexagonal phase and their morphology depend on

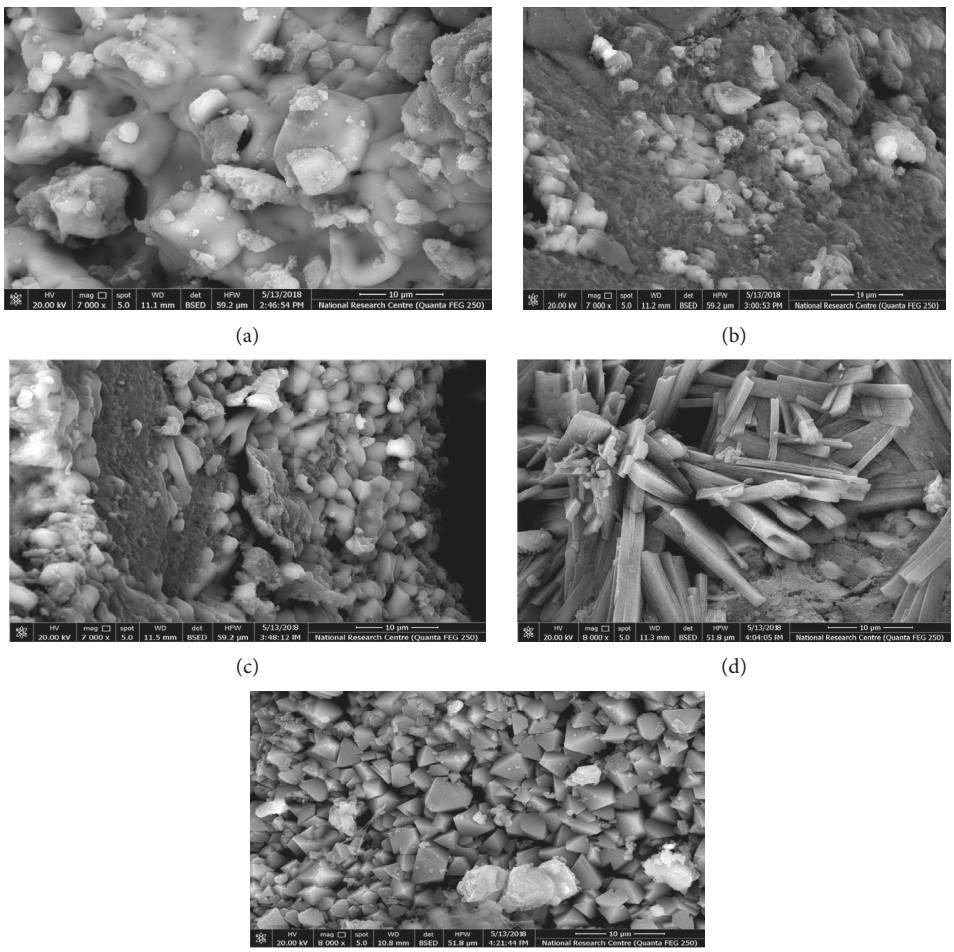

(a) (b) (c) (d) (e)

Figure 3: (a) SEM photo of prepared sample A. (b) SEM photo of prepared sample B. (c) SEM photo of prepared sample C. (d) SEM photo of prepared sample D. (e) SEM photo of prepared sample E.

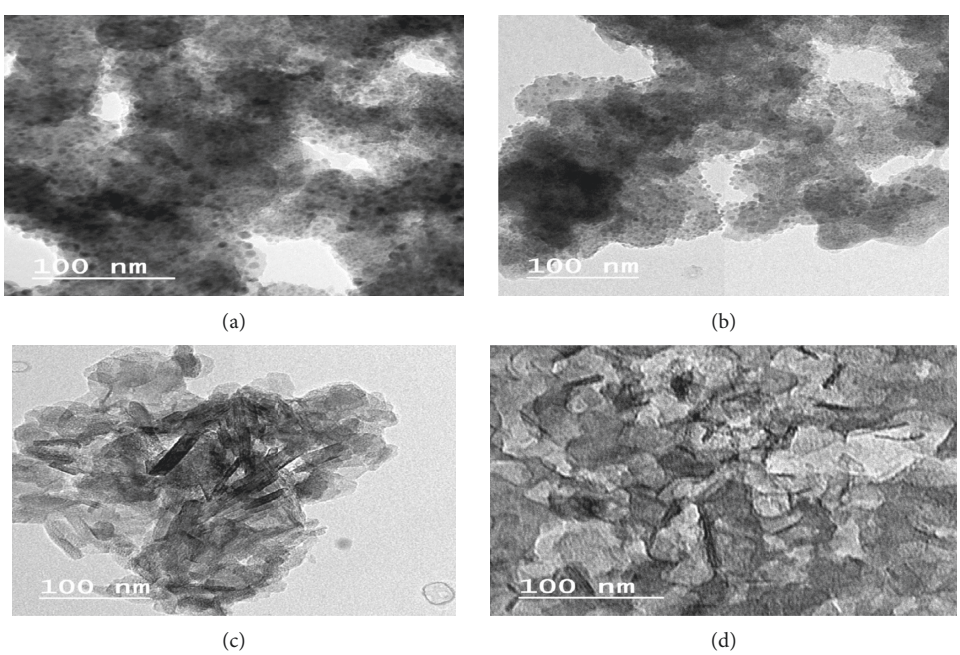

(a) (b) (c) (d)

Figure 4: Continued.

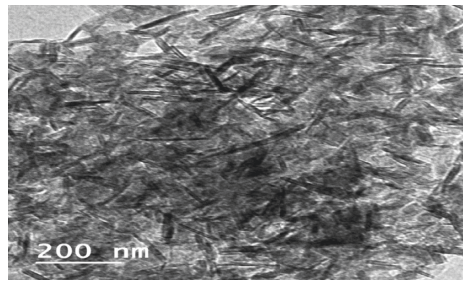

(e)

Figure 4: (a) TEM photo of prepared sample A. (b) TEM photo of prepared sample B. (c) TEM photo of prepared sample C. (d) TEM photo of prepared sample (D). (e) TEM photo of prepared sample E.

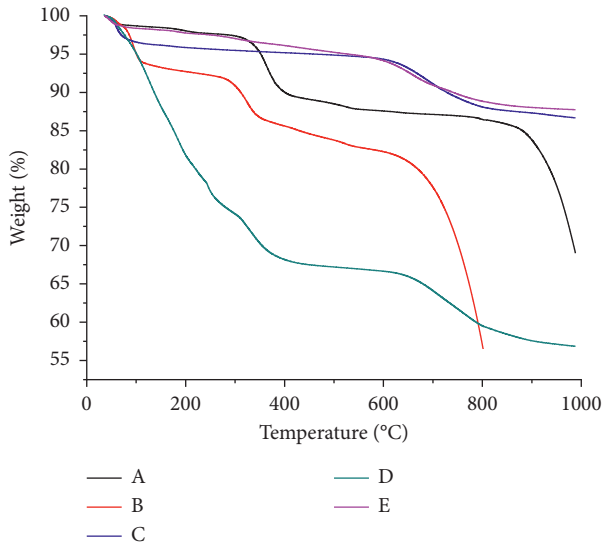

Figure 5: TGA of prepared samples.

the nature of the precursor materials when they are prepared by the same method. Also, it is observed that the prepared $Mg(OH)_2$ is thermally stable and by heating, it is converted to glassy layers and liberates water. The value of the glassy layer may be arranged as follows E > C > A > B > D. The obtained samples may be used as flame-retardant materials especially those prepared in presence of the surfactants.

Data Availability

The data used to support the findings of this study are available from the corresponding author upon request.

Conflicts of Interest

The authors declare that they have no conflicts of interest.

Acknowledgments

The authors gratefully acknowledge the National Research Center (NRC) for support and funding this work through the project AR 111904.

References

[1] A. Horrocks, "Textile flammability research since 1980—personal challenges and partial solutions," *Polymer Degradation and Stability*, vol. 98, pp. 2813–2824, 2013.

[2] A. R. Horrocks, "Flame retardant challenges for textiles and fibres: new chemistry versus innovatory solutions," *Polymer Degradation and Stability*, vol. 96, no. 3, pp. 377–392, 2011.

[3] S. Bourbigot, S. Duquesne, and C. Jama, "Polymer nanocomposites: how to reach low flammability?," *Macromolecular Symposia*, vol. 233, no. 1, pp. 180–190, 2006.

[4] B. Alexander and J. Gilman, "An overview of flame retardancy of polymeric materials: application, technology and future direction," *Fire and Materials*, vol. 37, no. 4, pp. 259–279, 2012.

[5] F. Laoutid, P. Gaudon, J.-M. Taulemesse, J. M. Lopez Cuesta, J. I. Velasco, and A. Piechaczyk, "Study of hydromagnesite and magnesium hydroxide based fire retardant systems for ethylene-vinyl acetate containing organo-modified montmorillonite," *Polymer Degradation and Stability*, vol. 91, no. 12, pp. 3074–3082, 2006.

[6] S. Ray and M. Okamoto, "Polymer/layered silicate nanocomposites: a review from preparation to processing," *Progress in Polymer Science*, vol. 28, pp. 1539–1641, 2003.

[7] C. Feng, Y. Zhang, D. Lang, S. Liu, C. Zhen-guo, and J. Xu, "Flame retardant mechanism of a novel intumescent flame retardant polypropylene," *Procedia Engineering*, vol. 52, no. 3, pp. 97–104, 2013.

[8] H.-Q. Yin, D. Yuan, and X.-F. Cai, "The high efficiency two stage intumescent-contractive flame retardant on ABS," *Polymer Degradation and Stability*, vol. 98, no. 1, pp. 288–296, 2013.

[9] J. Xin-Ke, G. De-Ming, J.-B Zhang et al., "Thermal transition behavior, thermal stability, and flame retardancy of low-melting-temperature copolyester: comonomer effect," *Industrial & Engineering Chemistry Research*, vol. 52, no. 12, pp. 4539–4546, 2013.

[10] S. Mer, M. Mugla, and P. Huseyin, "Effect of SiO_2 and Al_2O_3 nano particlees treatment on thermal behavior of oriental beech wood," *Composite*, vol. 4, pp. 573–582, 2018.

[11] Y. Zhang, J. Chen, and A. Song, "Two-step preparation of magnesium hydroxide flame retardant from magnesium oxide," *Chinese Journal of Inorganic Chemistry*, vol. 30, pp. 860–866, 2014.

[12] J. Lv, L. Qiu, and B. Qu, "Controlled synthesis of magnesium hydroxide nanoparticles with different morphological structures and related properties in flame retardant ethylene-vinyl

acetate blends," *Nanotechnology*, vol. 15, no. 11, pp. 1576–1581, 2004.

[13] Y. Hu and S. Li, "The effects of magnesium hydroxide on flash pyrolysis of polystyrene," *Journal of Analytical and Applied Pyrolysis*, vol. 78, no. 1, pp. 32–39, 2007.

[14] L. Xue, S. Tongxin, C. Peng, and L. Yunyi, "Preparation of magnesium hydroxide flame retardant from light calcined powder by ammonia circulation method," *Powder Technology*, vol. 260, pp. 98–104, 2014.

[15] C. Yan, D. Xue, L. Zou, X. Yan, and W. Wang, "Preparation of magnesium hydroxide nanoflowers," *Journal of Crystal Growth*, vol. 282, no. 3-4, pp. 448–454, 2005.

[16] C. Yongbin, Z. Tao, F. Huaxiong, L. Simin, Y. Yuting, and H. Yang, "Anovel preparation of nano sized hexagonal $Mg(OH)_2$," *Procedia Engineering*, vol. 102, pp. 388–349, 2015.

[17] C. Henrist, J.-P. Mathieu, C. Vogels, A. Rulmont, R. Cloots, and R. Cloots, "Morphological study of magnesium hydroxide nanoparticles precipitated in dilute aqueous solution," *Journal of Crystal Growth*, vol. 249, no. 1-2, pp. 321–330, 2003.

[18] J. Wenjun, H. Xiao, H. Qiaofeng, Y. Xujie, L. Lude, and W. Xin, "Preparation of lamellar magnesium hydroxide nano-particles via precipitation method," *Powder Technology*, vol. 191, no. 3, pp. 227–230, 2009.

[19] G. Pachler, F. Matlok, and H. Gremlich, *Merck FTIR Atlas: A Collection of FTIR Spectra*, Weineim, New York, NY, USA, 1988.

[20] H. Dong, Z. Du, Y. Zhao, and D. Zhou, "Preparation of surface modified nano-$Mg(OH)_2$ via precipitation method," *Powder Technology*, vol. 198, no. 3, pp. 325–329, 2010.

[21] H. Yang, F. Li, C. Shan et al., "Covalent functionalization of chemically converted graphene sheets via silane and its reinforcement," *Journal of Materials Chemistry*, vol. 19, no. 26, pp. 4632–4638, 2009.

[22] Y. Tian, G. Wang, F. Li, and D. G. Evans, "Synthesis and thermo-optical stability of o-methyl red-intercalated Ni-Fe layered double hydroxide material," *Materials Letters*, vol. 61, no. 8-9, pp. 1662–1666, 2007.

[23] Y. Li, M. Sui, Y. Ding, G. Zhang, J. Zhuang, and C. Wang, "Preparation of $Mg(OH)_2$ nanorods," *Advanced Materials*, vol. 12, no. 11, pp. 818–821, 2000.

[24] X.-F. Wu, G.-S. Hu, B.-B. Wang, and Y.-F. Yang, "Synthesis and characterization of superfine magnesium hydroxide with monodispersity," *Journal of Crystal Growth*, vol. 310, no. 2, pp. 457–461, 2008.

[25] X.-Z. Tang, W. Li, Z.-Z. Yu et al., "Enhanced thermal stability in graphene oxide covalently functionalized with 2-amino-4,6-didodecylamino-1,3,5-triazine," *Carbon*, vol. 49, no. 4, pp. 1258–1265, 2011.